Distribution Agreement

In presenting this thesis as a partial fulfillment of the requirements for a degree from Emory University, I hereby grant to Emory University and its agents the non-exclusive license to archive, make accessible, and display my thesis in whole or in part in all forms of media, now or hereafter now, including display on the World Wide Web. I understand that I may select some access restrictions as part of the online submission of this thesis. I retain all ownership rights to the copyright of the thesis. I also retain the right to use in future works (such as articles or books) all or part of this thesis.

Henry Blair April 4th, 2023

Altered functional connectivity of the anterior insula in attention networks:

Implications for female children with autism spectrum disorder

By

Henry Blair

Opal Ousley, Ph.D.
Advisor

Neuroscience and Behavioral Biology

Opal Ousley, Ph.D.
Advisor

Gillian Hue, Ph.D.
Committee Member

James Rilling, Ph.D.
Committee Member

2023

Altered functional connectivity of the anterior insula in attention networks: Implications for female children with autism spectrum disorder

By

Henry Blair

Opal Ousley, Ph.D.
Advisor

An abstract of
a thesis submitted to the Faculty of Emory College of Arts and Sciences
of Emory University in partial fulfillment
of the requirements of the degree of
Bachelor of Science with Honors

Neuroscience and Behavioral Biology

2023

Abstract

Altered functional connectivity of the anterior insula in attention networks:
Implications for female children with autism spectrum disorder

By

Henry Blair

Although the anterior insula has been investigated in autism spectrum disorder for some time, there are conflicting findings about its functional connectivity. This project looks at sex independently and examines the functional connectivity between the anterior insula and various regions within the salience network and ventral attention network. We use ROI-to-ROI analyses to assess functional connectivity between the AI and regions of these two networks. All scans were preprocessed in a standard fashion, allowing us to perform connectivity analyses. Results demonstrated that there are significant differences in connectivity patterns between these networks and the anterior insula in autistic children - particularly within the temporoparietal junction and supramarginal gyrus. The increased connectivity within autistic females and decreased connectivity in autistic males highlight the importance of factoring sex into analyses on autism and in research on other developmental conditions. The preliminary results correlating resting-state functional connectivity in autistic females to autism symptom scores provide an example of how resting-state connectivity between the AI and VAN regions can be useful for estimating a patient's behavioral symptoms or severity of autism.

Keywords: functional connectivity, sex difference, anterior insula, autism spectrum disorder, temporoparietal junction

Altered functional connectivity of the anterior insula in attention networks: Implications for female children with autism spectrum disorder

By

Henry Blair

Opal Ousley, Ph.D.
Advisor, Committee Member

A thesis submitted to the Faculty of Emory College of Arts and Sciences
of Emory University in partial fulfillment
of the requirements of the degree of
Bachelor of Sciences with Honors

Neuroscience and Behavioral Biology

2023

Table of Contents

Introduction:

Autism spectrum disorder (ASD) is a neurodevelopmental disorder characterized by early dysfunction in social interactions, repetitive behaviors, and atypical interest. Around 2.7% of children in the US have ASD (Shaw et al., 2023), and estimates suggest that there are both genetic (Yoo et al., 2015) and environmental (Reis et al., 2021) contributions to its development in children.

Although ASD has been studied for a very long time, there has been limited research on females. Historically speaking, autism has been thought of as a predominantly male disorder, which may contribute underdiagnosing in females (Lai et al., 2016). Currently, autism is diagnosed in 1:36 children and is reported about four times more often in boys than girls (Shaw et al., 2023). However, some have attributed this disparity between diagnoses in the sexes to a differential presentation of autistic traits, and many have purported that increased social "masking," or increased inhibition of natural tendencies which are characteristic of autism, may contribute to the lower frequency of diagnosis in females (Rynkiewicz et al., 2016; Schuck et al., 2019). However, the prevalence of autism has increased over the past few decades and scientists are beginning to look at sex as a variable within autism (Dougherty et al., 2022).

The anterior insula (AI) has been associated with self-awareness, pain, social behavior, social and emotional cognition, and has been implicated with social differences in autism, such as reduced eye contact, atypical attention, and poor empathy (Caria and de Falco, 2015). Recent studies have discovered that the optogenetic activation of the AI in rats leads to suppression of the default mode network (DMN) and simultaneous activation of the salience network (SN) (Menon et al., 2023). The SN is responsible for salience detection, which is critical for producing appropriate behaviors in response to relevant stimuli. Atypical salience detection and SN activity

has been reported numerous times in ASD (Bishop-Fitzpatrick et al., 2016, Loomba et al., 2021, Guo et al., 2018). Salience detection involves bottom-up processing via the ventral attention network (VAN), or the control of focus when many irrelevant stimuli compete for one's attention (Fitzgerald et al., 2014).

The VAN is thought to reorient attention toward an exogenous or unexpected stimulus and acts as a circuit breaker for the dorsal attention network. The VAN works in tandem with the SN in controlling attention across multiple stimuli and, in particular, reorienting of attentions (Touroutoglou et al., 2016). Like the SN, resting-state functional connectivity (RSFC) analyses have shown atypical patterns in the VAN of autistic individuals (Farrant and Uddin, 2016; Hull et al., 2018). A central finding which inspired this project is that the AI is linked to the VAN both structurally, as measured by diffusion tensor imaging (DTI), and functionally, as measured via functional magnetic resonance imaging (fMRI) (Klugah-Brown et al., 2021). Like the SN, recent studies have also found increased connectivity in the VAN regions in individuals with ASD (Jung et al., 2018).

As sex has been investigated in autism recently, sex differences in salience network connectivity are beginning to be established (Tavares et al., 2021). Notably, one study found that relative to female children with ASD, the autistic male children had a stronger association between sensory over-responsivity and the increased functional connectivity (FC) between the salience and primary sensory networks that was observed when contrasting functional scans to sex-matched controls. (Cummings et al., 2020; Lawrence et al., 2020; Lawrence et al., 2022). This may imply an increased allocation of attention toward sensory information within autistic males. On the other hand, the autistic females in this study had a stronger association than autistic males between sensory over-responsivity and the increased FC from the SN to the prefrontal cortex that was

observed when both groups were contrasted to sex-matched controls. (Cummings et al., 2020; Lawrence et al., 2020; Lawrence et al., 2022). Additionally, another recent study found increased structural covariance in autistic male children of 2 to 4 years of age but decreased structural covariance in autistic females when compared to age- and sex-matched controls (Zielinski et al., 2022). Although structural covariance MRI measures morphological properties (i.e., gray matter volume or cortical thickness), something completely different from the blood-oxygen-level-dependent (BOLD) signal in functional connectivity MRI (fcMRI), structural covariance analyses demonstrate that there are qualitative and quantitative differences in how autism manifests in males and females. Moreover, while autistic males have reduced RSFC in the salience network and increased RSFC in the dorsal attention network, females with autism have reduced RSFC in the DMN and increased RSFC in the dorsal attention network (Alaerts et al., 2016).

We aim to determine how the AI's connectivity with the SN and VAN is atypical in ASD. The SN includes the anterior cingulate cortex (ACC), insular cortex (IC), lateral prefrontal cortex (LPFC), precuneus, posterior cingulate cortex (PCC), the supramarginal gyrus (SMG), rostral prefrontal cortex (RPFC), and frontal operculum (FO) (Yerys et al., 2020; RPFC link). The VAN consists predominantly within the right hemisphere (Downar et al., 2000) and it involves the ventral frontal cortex (VFC), the AI, the middle and inferior frontal gyri, and the temporoparietal junction (TPJ), which is made up of the superior temporal gyrus (STG), angular gyrus (AG), and middle temporal gyrus (MTG) (Schulman et al., 2006; Onofrj et al., 2022).

One study correlated the decreased connectivity of the SN to the severity of restricted and repetitive behaviors, symptoms of ASD in children who were 8.5 to 10.4 years of age (Uddin et al., 2013; Uddin and Menon, 2009). Because of the AI's role in the SN and VAN, the established atypical connectivity in ASD, and the association to autism symptoms, we hypothesized that

compared to TD subjects, ASD subjects will exhibit increased connectivity between AI and the aforementioned networks. This may relate to the difficulty in adapting to change in ASD, restrictive and repetitive behaviors (Leekam et al., 2011), and increased sensitivity to sensory stimuli (Baron-Cohen et al., 2009).

Although sex-differences in ASD are known but not well established. One study reported that autistic females exhibited increased connectivity where autistic males exhibited decreased connectivity when compared to their counterparts (Alaerts et al., 2016). However, this work did not focus within the SN and VAN. Autism has primarily been thought of as "male disorder" (Lai et al., 2016). Autism is currently 4x more common in males (Shaw et al., 2023) and although its prevalence has increased the past few decades (Dougherty et al., 2022), there is still much research to be done comparing how RSFC relates to the differential presentation of autistic traits in each sex. We use sex as a variable to examine its impact on autism's effect on the RSFC between the AI and the SN and VAN.

Four studies that we reviewed examined the relation between symptom severity and the RSFC of the AI and SN or VAN. In a sample of children with and without autism aged 8.5 to 10.4 years, connectivity was used to estimate restricted and repetitive behavior scores, as measured by the Autism Diagnostic Interview - Revised (ADI-R), but the data was unable to estimate other ADI-R scores (Uddin et al., 2013). A work looking at the dorsal AI found increased connectivity to the TPJ which showed negative correlations with the ADI-R Onset Total score (Odriozola et al., 2015). A seminal paper investigating the difference in the RSFC of insular subregions observed hypoconnectivity between granular regions of the insula and the right SMG and were able to correlate this with severity (Xu et al., 2018). However, this study used only 9 females total out of 82 subjects) and it did not look at differences in connectivity with sex independently. The most

recent study seeking to determine how FC of the insula relates to severity was examining connectivity between the SN and the occipital-temporal face network (Pua et al., 2020). This investigation found that increased connectivity related to severity as measured by SRS scores. However, this study included no females in their sample of 160 children with or without autism. Thus, we predict that FC alterations in autistic females (compared to typically developing females) will significantly correlate to severity.

To our knowledge, no study has used sex as a variable while focusing solely on the RSFC AI with SN and VAN, compared the effects of autism on FC in each sex, examined the relation between patterns in FC and severity of autism, and included at least 10 females in severity analyses. Thus, our approach is novel.

Specific Hypotheses:

The study will examine three hypotheses. (1) We hypothesize that ASD subjects will exhibit greater connectivity (ASD > TD) between the AI and regions that are part of the salience and ventral attention networks. The SN regions we are investigating include the anterior cingulate cortex (ACC), the precuneus, the posterior cingulate cortex (PCC), the supramarginal gyrus (SMG), parietal operculum (PO) and the frontal operculum (FO). The VAN regions we are examining include the ventral frontal cortex (VFC) which consists of the middle and inferior frontal gyri (MFG, IFG) and the temporoparietal junction (TPJ) which consists of the superior temporal gyrus (STG), middle temporal gyrus (MTG), and the angular gyrus (AG). (2) We will also repeat the analyses above while looking at sex as a variable; we expect to find sex differences in AI connectivity to the SN and the VAN. (3) As an exploratory aim, we will investigate the relation between connectivity patterns in autistic females and their symptom scores for ASD. We will not be looking at RSFC patterns in autistic males and its relation to symptom scores for ASD

due to time constraints. However, this will be a post-hoc analysis (along with many others) to be performed before finishing the results section of this paper and submitting for publication.

Methods:

Subjects:

Our project relies on one of the largest open-source autism datasets, allowing for the examination of connectivity within one age group and comparing between the two genders. All data were acquired from the open-source Autism Brain Imaging Data Exchange I dataset (ABIDE I) via the Collaborative Informatics and Neuroimaging Suite (COINS). A total of 184 scans (92 functional scans, 92 structural scans) were downloaded from the ABIDE I database. These scans were collected at two institutions and came from 92 subjects who were eight to twelve years old (TD = 47, ASD = 45). Included in this dataset are 20 females (TD = 13, ASD = 7) and 72 males (TD = 34, ASD = 38), with the mean ages of for females was 10.08 (SD = 1.59) and 10.39 (SD = 1.22), respectively. This data is unique given its focus on school age children which is younger than many fMRI studies investigating autism.

Assessments:

We are comparing these connectivity measures with the scores of each subject on the Social Responsiveness Scale, Version 2 (SRS™-2), Module 3 of the Autism Diagnostic Observation Schedule™, the Second Edition (ADOS™-2), the Social Communication Questionnaire (SCQ), and the Autism Diagnostic Interview - Revised (ADI-R). The use of the Module 3 of ADOS™-2 requires that individuals are verbally fluent. An additional ADOS-2 Gotham-Calibrated Total score, derived from ADOS™-2, was also used (Gotham et al., 2008) and is labeled AGT in the table below. Measurements for full IQ, performance IQ, and verbal IQ were also included. Each

of these assessments were included when we downloaded our data from the ABIDE I database and are common tools used to diagnose autism. Collectively, these assessments take into account restricted repetitive behaviors, social communication and interaction skills, and other factors that are relevant for diagnosing a child with autism (Gotham et al., 2006; Chan et al., 2017; Gotham et al., 2008). We use these assessments to examine the relation between connectivity and symptom scores in autistic females.

Table 1: Subject Assessment Measures

ASD (N = 45)									
Measure or Score	*Males (N=38)*			Females (N = 7)			M-F Sex Difference		
	N	Mean	SD	N	Mean	SD	t-value	p-value	cohen's d
Age	38.00	10.26	1.17	7.00	10.36	1.53	-0.20	0.84	0.01
FIQ	38.00	106.68	18.29	7.00	108.14	19.88	-0.19	0.85	0.01
VIQ	38.00	105.00	16.74	7.00	111.14	19.84	-0.19	0.85	0.06
PIQ	38.00	108.58	19.27	7.00	102.71	17.49	0.75	0.46	0.05
AGT	38.00	12.37	5.10	7.00	11.86	5.90	0.24	0.81	0.02
ADI-R Social	37.00	19.84	5.28	7.00	20.43	6.68	-0.26	0.80	0.02
ADI-R Verbal	37.00	15.76	4.23	7.00	17.57	5.06	-1.01	0.32	0.07
ADI-R RBB	37.00	5.41	2.51	7.00	5.71	2.87	-0.29	0.77	0.02
SRS Total	36.00	88.67	28.69	7.00	103.86	38.12	-1.22	0.23	0.09
SCQ	27.00	15.33	6.71	4.00	20.25	6.85	-1.36	0.18	0.14

TD (N = 47)									
Measure or Score	Males (N = 34)			Females (N =13)			M - F Sex Difference		
	N	Mean	SD	N	Mean	SD	t-value	p-value	cohen's d
Age	34.00	10.55	1.27	13.00	9.93	1.66	-1.36	0.18	0.08
FIQ	34.00	111.62	14.32	13.00	113.92	16.61	0.47	0.64	0.03
VIQ	34.00	111.24	13.71	13.00	114.23	15.57	0.65	0.52	0.04
PIQ	34.00	109.15	14.74	13.00	111.23	15.86	0.42	0.67	0.02
AGT	x	x	x	x	x	x	x	x	x
ADI-R Social	x	x	x	x	x	x	x	x	x
ADI-R Verbal	x	x	x	x	x	x	x	x	x
ADI-R RBB	x	x	x	x	x	x	x	x	x
SRS Total	32.00	21.13	17.66	13.00	20.62	12.05	-0.10	0.92	0.01
SCQ	9.00	4.33	2.24	5.00	1.80	0.84	-2.40	0.03 *	0.40

Measure or Score	ASD ALL (N = 45)			TD ALL (N = 47)			ASD-TD Difference		
	N	Mean	SD	N	Mean	SD	t-value	p-value	cohen's d
Age	45.00	10.27	1.21	47.00	10.37	1.40	-0.38	0.71	0.01
FIQ	45.00	106.91	18.32	47.00	112.26	14.84	-1.54	0.13	0.04
VIQ	45.00	105.96	17.16	47.00	112.06	14.14	-1.87	0.07	0.05
PIQ	45.00	107.67	18.94	47.00	109.72	14.91	-0.58	0.56	0.02
AGT	45.00	12.29	5.16	x	x	x	x	x	x
ADI-R Social	44.00	19.93	5.44	x	x	x	x	x	x
ADI-R Verbal	44.00	16.05	4.36	x	x	x	x	x	x
ADI-R RBB	44.00	5.45	2.54	x	x	x	x	x	x
SRS Total	43.00	91.14	30.43	45.00	20.98	16.11	13.60	0.00 ***	0.36
SCQ	31.00	15.97	6.82	14.00	3.43	2.21	6.68	0.00 ***	0.34

Note: Comparison of phenotypic variables downloaded and assessed in this project. No significant differences between the autistic males and autistic females were observed. The only difference between TD males and TD females was for the SCQ score. Autistic and typically developing subjects differed significantly for the SRS-2 raw total score, the SCQ score. (*,

indicates a p-value < 0.05, *** p-value < 0.001; Actual p-values SRS-2 [SCQ] are 3.76×10^{-23} [3.72×10^{-08}]). Values of "x" indicate that an assessment was not given for a particular group. Legend: full intelligence quotient (FIQ), performance intelligence quotient (PIQ), and verbal intelligence quotient (VIQ), Gotham-Calibrated Autism Diagnostic Observation Schedule Total Score (AGT), the social (ADI-R Social), verbal (ADI-R Verbal), restrictive and repetitive behaviors (ADI-R RBB) sub-scores for the Autism Diagnostic Interview - Revised (ADI-R), the Social Responsiveness Scale Total Score (SRS Total), and the Social Communication Questionnaire (SCQ).

As indicated in Table 1, there were no significant differences between autistic males and autistic females. Typical males had SCQ scores that were significantly higher than typically developing females. A greater score implies greater tendencies for behaviors that are characteristic of autism. However, the SCQ score is not a diagnostic tool. The SCQ is an assessment commonly used to screen for ASD. A threshold cutoff score of 15 which is commonly used to determine if further evaluation is needed to diagnose a child or rule out a diagnosis (Berument et al., 1999). The TD male mean of 4.33 does not near the threshold cutoff score of 15. The ASD group had a significantly larger score for the SRS-2 Raw Total and the SCQ as expected with their diagnosis. This indicates a strong difference between the two groups and validates that our sample was appropriate for each group.

Neuroimaging:

All scans were performed on a SIEMENS MAGNETOM Allegra syngo MR 2004A with TR = 2000 ms, interleaved ascending slice order, and field strength of 3 Tesla. Each subject received one functional and one anatomical scan. All scans were collected at either NYU or Yale using these parameters, and all scans were acquired from the ABIDE I database.

Preprocessing:

All preprocessing was completed through the Statistical Parametric Mapping, Version 12 (SPM12) software on MatLab (R 2022b). All preprocessing was done via a script which followed

the same steps as the "Default Preprocessing Pipeline" on CONN Toolbox (Nieto-Castanon, 2020). This script can be made available upon request. ~~Preprocessing is a necessary part of all fMRI projects as each scan must be transformed and standardized in stereotaxic space like the Montreal Neurological Institute (MNI) coordinate system before analysis can occur. Subjects may move their heads during scans, and individuals may have different cortical volumes and shapes. Thus, in order to analyze fMRI data, these and many other variables must be standardized.~~

Realignment: Estimate and Reslice: Subjects with movement over ± 3 mm range or rotation over ± 3º in any direction were excluded from the study, as this is the standard for fMRI scans of children (Hagen et al., 2012). For the remaining subjects, to correct for head motion, realignment of each fMRI volume to a reference volume was performed. Motion can distort the magnetic field that has been set up for a particular head position, which is an issue because the magnetic field is critical for creating the images of brain activity, and any distortion can lead to errors in the data. Additionally, motion can cause the brain to shift into different parts of the brain within the same scan which can lead to mismatches between functional data and anatomical data, which obscures the identification of specific brain regions associated with neural activity. By realigning, we minimized this effect.

Coregistration: Estimate and Reslice: Functional scans were overlaid onto an anatomic reference scan of the same subject.

Slice timing: Because fMRI volumes are produced by stacking a series of 2D images of the brain (like pancakes), slice timing correction calculates a transformation to realign all the images, which would otherwise be temporally misaligned.

Segmentation and Realignment: All scans were normalized to a standard space, allowing for standardized comparison and the removal of non-brain areas in images like the skull, scalp, and other non-brain tissue. This is important because these non-brain areas can cause artifacts in the images and lower the accuracy of the data. Next, we were warped to the IXI 549 MNI template so

that their BOLD responses could be compared.

Smoothing: Lastly, all functional images were smoothed using an 8mm isotropic Gaussian kernel to increase the signal-to-noise ratio.

Denoising:

In addition, functional data were denoised using a standard denoising pipeline (Nieto-Castanon, 2020) including the regression of potential confounding effects such as white matter timeseries (5 CompCor noise components), CSF timeseries (5 CompCor noise components), motion parameters (12 factors), outlier scans (below 39 factors) (Power et al., 2014; Power et al., 2017), and first order derivatives of motion (12 factors, or 3 rotations, 3 translations and their first order derivatives) (Friston et al., 1996). We applied bandpass frequency filtering of the BOLD time series between 0.008 Hz and 0.09 Hz (Hallquist et al., 2013). The effective degrees of freedom of the BOLD signal after denoising ranged from 37.7 to 56.1 across all subjects (Nieto-Castanon, 2020).

Creating ROIs:

We examined ROIs using the masks in the CONN toolbox (Nieto-Castanon, 2020) and the Wake Forest University (WFU) PickAtlas (Maldjian et al., 2003), including left, right, and bilateral regions of the SN (i.e., ACC, INS, LPFC, MFG, Precuneus, PCC, SMG, RPFC, FO, PO) and the VAN (i.e., AI, VFC - MFG + IFG, and TPJ - STG + MTG). Within the WFU PickAtlas, we used the IBASPM71 and IBASPM 116 atlases for left and right masks, and for bilateral masks, we used the TD Label Atlas (Lancaster et al., 1997) in addition to these atlases. These ROIs are labeled in Table 2. The frontal operculum, although very close to the AI, is not labeled in any of these atlases, so we used MNI coordinates to create 10 mm spheres for this region. We also made a mask for the

left, right and bilateral anterior insula because CONN's seed was not centered around the coordinates identified in the most relevant previous literature. We visually inspected the AI mask to ensure it was consistent with the region we were targeting. The seeds for these regions are listed in Table 3 and based on prior work (Iuculano et al., 2020; Allen et al., 2016; Bonelle et al., 2012).

Table 2: ROIs created for connectivity analyses for targets of the VAN and the SN

Ventral Attention Network ROIs	Salience Network ROIs
TPJ (STG, MTG, AG)	LPFC (MFG)
STG	IC
MTG	SMG
AG	PCC
AI	Precuneus
Whole IFG	ACC
IFG pars opercularis	FO
IFG pars orbitalis	PO
IFG pars triangularis	RPFC

Note: ROIs created with the SPM12 WFU PickAtlas package using the IBASPM71 and IBASPM 116 atlases. A left, right, and bilateral mask was generated for each ROI.

Table 3: MNI Coordinates for the ROIs not labeled in IBASPM atlases

Ventral Attention Network MNI Coordinates for ROIs not labeled in atlases				
ROI	Left	Right	Bilateral	Source
AI (1)	- 36, 18, -6	+ 36, 18, -6	± 36, 18, -6	Iuculano et al., 2020
AI (2)	- 36, 20, 1	+ 36, 20, 1	± 36, 20, 1	Allen et al., 2016
AI (3)	- 36, 24, -6	+ 36, 24, -6	± 36, 24, -6	Bonnelle et al., 2012
FO	- 56, 14, 14	+ 56, 14, 14	± 56, 14, 14	McMenamin et al., 2014

Note: Table 3 Description: Seeds used to create masks of the AI and the frontal operculum (FO).

1st level ROI-to-ROI Connectivity Analysis

We estimated ROI-to-ROI connectivity matrices characterizing the RSFC between each pair of regions among all ROIs. We used Fisher-transformed bivariate correlation coefficients from a general linear model to represent RSFC strength, and individual scans were weighted using a linear regression that regressed the signal intensity of each scan against the mean signal intensity and motion parameters. Regression coefficients are used as weights so that all scans contribute equally to the analysis (Nieto-Castanon, 2020). The weighting of individual scans was done because changing the magnetic field in the scanner during the scan can cause transient magnetization effects that cause some scans to have stronger or weaker signals than others, which can affect the accuracy or the reliability of subsequent connectivity analyses (Nieto-Castanon, 2020).

2nd Level Group Connectivity Analysis

For group-level analyses, we used a General Linear Model (Nieto-Castanon, 2020b) to estimate each individual connection. To investigate the RSFC between a seed ROI and another target ROI, connection-level hypotheses were evaluated using bivariate correlation statistics with random-effects across groups and sample covariance estimation across multiple measurements (Nieto-Castanon, 2020a). We used hemodynamic response function (HRF) weighting to improve the accuracy of our connectivity values, as has been established by previous studies. The BOLD signal is slow and delayed, so the HRF function adjusts it to improve the temporal relationship between brain regions. This is done by convolving the HRF model with the time series for each voxel and subsequently normalizing the result to reduce the impact of inter-subject variability in BOLD signal intensity by scaling the weighted connectivity values for each subject. Normalization of the BOLD signal is dividing connectivity values by the average connectivity across the whole brain for each subject. This adjusts the connectivity values, so they are more comparable across

subjects, which prevents differences in functional connectivity resulting from individual differences in BOLD signal intensity.

Some have reported that HRF weighting improved the accuracy of FC estimates in resting-state data (Prokopiou et al., 2020), like ours. Additionally, others have reported that HRF weighting improved the accuracy of RSFC estimates, reduced the impact of head motion in child samples (Saad et al., 2022), and improved the specificity of group differences in connectivity measures between autistic and typically developing individuals (Power et al., 2017; Van Dijk et al., 2012; Anderson et al., 2011; Ye et al., 2020). Inferences were performed at the level of individual ROIs. ROI-to-ROI connectivity results were thresholded using a combination of a $p < 0.05$ connection-level threshold and a familywise corrected p-FDR < 0.05 ROI-level threshold (Benjamin and Hochberg, 1995), where the time series for all voxels within each ROI were averaged and connectivity was based on connectivity between ROIs rather than on the clustering of voxels.

Connectivity to Severity Analyses

To determine how the altered connectivity related to ASD symptom scores in females, we used CONN Toolbox's Calculator tool to perform a linear regression between connectivity values (between two regions) and three assessments as measures of severity: the SRS-2 Raw Total scores, SCQ Total Scores, and ADI-R Onset Total Scores. For each subject, connectivity values between were recorded that corresponded to the strength and direction of connectivity that was altered in autistic females compared to typically developing females. These connectivity values for each subject were subsequently applied to a linear regression model to estimate the

relationship between connectivity values and the variable of interest (SRS-2, SCQ, and ADI-R symptom scores).

Results:

To investigate differences in RSFC in autistic males, a [1, -1] contrast against TD males was used. This contrast is the standard method to calculate between-group differences in fcMRI analyses. The "1" condition refers here to ASD subjects, and the "-1" condition refers to TD subjects. An individual's beta value represents the strength of connection between two brain regions. For each ROI target, the beta values of all individuals are averaged to calculate a group's beta value, which is subsequently multiplied by their contrast values to evaluate a group difference. If the beta value is positive, this suggests that the RSFC between the right/left AI and the target ROI is stronger in the first group than in the second. If the beta value is negative, this suggests that the RSFC between the two regions is weaker in the first group than in the second, or decreased connectivity. For example, if the beta value for an ROI in the ASD group is 0.2 and the corresponding beta value in the TD group is 0.3, then the difference in RSFC between the two groups is -0.1, which is calculated as (0.2 x 1) - (0.3 x -1) = -0.1. This negative value indicates that the RSFC in this ROI is lower in the ASD group compared to the TD group. Therefore, the beta values in this case represent both the strength of the connection between two brain regions (RSFC values) and the difference in RSFC between the ASD and TD groups. By applying the contrast values [1, -1] to these beta values, you can obtain a measure of the magnitude and direction of the between-group differences in RSFC. We predicted that autistic subjects would display increased connectivity (positive group beta values) between the AI and the regions of the SN and VAN.

Figure 1: Connectivity of the right AI to the SN and VAN in males

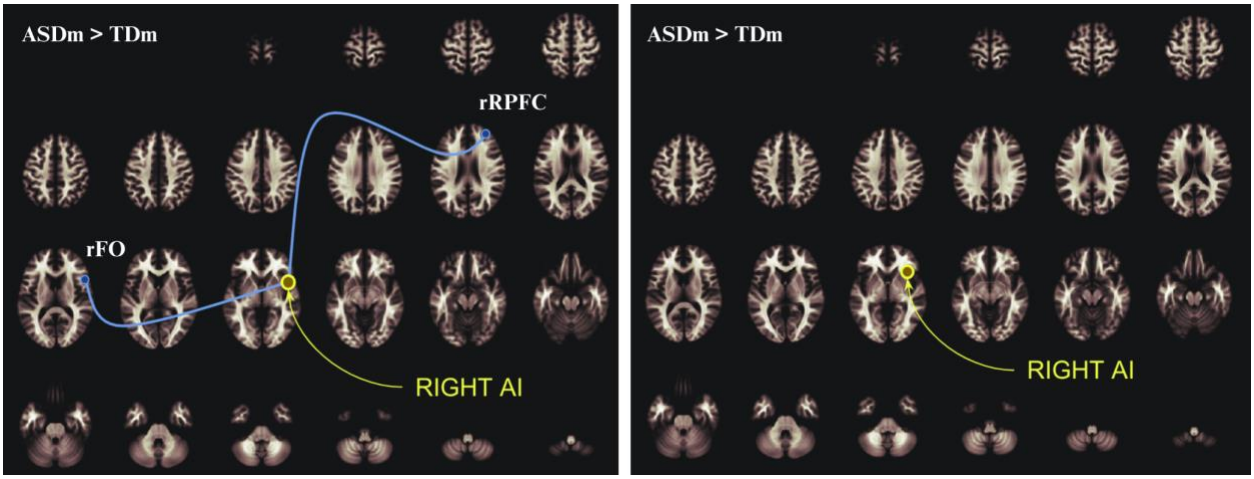

Note: Autistic male increased connectivity (ASDm > TDm) is shown in red (none) and decreased connectivity (ASDm < TDm) is shown in blue. Significant connectivity using CONN's right AI ROI seed centered at 47,14,0 (1a, left) and right AI mask (1b, right) as defined in Table 3.

Figure 2: Connectivity of the left AI to the SN and VAN in males

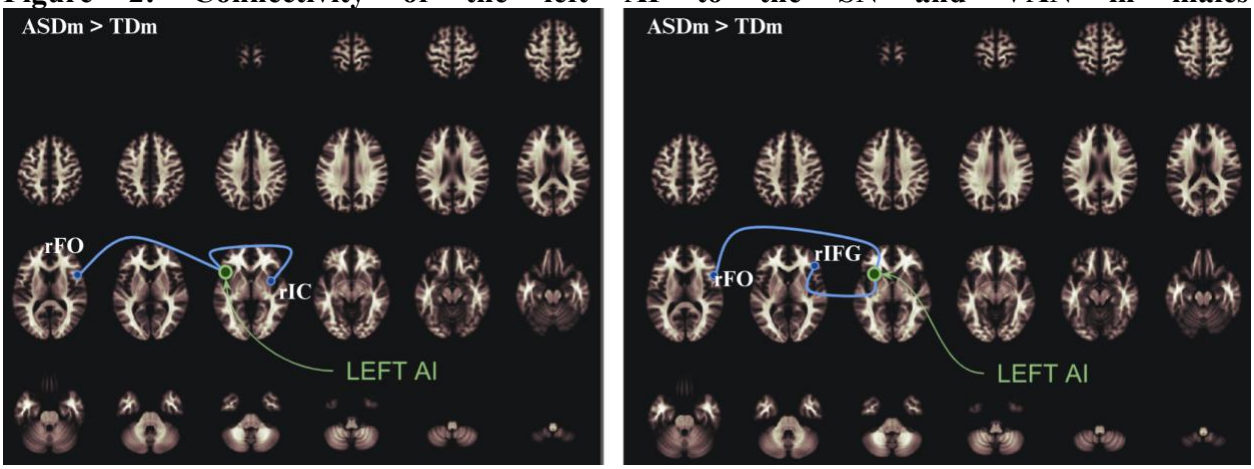

Note: Autistic male increased connectivity (ASDm > TDm) is shown in red (none) and decreased connectivity (ASDm < TDm) is shown in blue. Connectivity from CONN's left AI ROI seed centered at -44,13,0 (2a, left) and left AI mask (2b, right) as defined in Table 3.

The results of this study suggest significant decreased connectivity between the right AI and the right FO and right RPFC in autistic males (Figure 1a, Table 4). Weaker connectivity patterns were observed in autistic males between the left AI and the right FO (2a and 2b), right IC (2a), and the right IFG (2a) (Figure 2, Table 4). Stronger connectivity was not observed in autistic males compared to TD males between either AI and any target in the SN or VAN.

Table 4: Summary of Results in Figures 1 and 2, altered connectivity in autistic males compared to typically developing males.

ASDm > TDm	Contrast: 1, -1				
Targets with significant differences in connectivity with the *right* AI (mask or conn's seed):					
Hyperconnectivity in ASD	beta	t-value	p-uncor.	p-FDR	Ntwk
None					
Hypoconnectivity in ASD					
FO (R)	-0.11	-2.07	0.041723	0.843881	SN
RPFC (R)	-0.12	-2.05	0.044001	0.843881	SN

ASDm > TDm	Contrast: 1, -1				
Targets with significant differences in connectivity with the *left* AI (mask or conn's seed):					
Hyperconnectivity in ASD	beta	t-value	p-uncor.	p-FDR	Ntwk
None					
Hypoconnectivity in ASD					
FO (R)	-0.15	-2.45	0.016688	0.899046	SN
† IC (R)	-0.12	-2.06	0.043535	0.848363	SN
† FO (R)	-0.13	-2.04	0.045438	0.848363	SN
IFG (R)	-0.1	-2.01	0.048172	0.899046	VAN

† ⇒ connectivity with conn's seed for anterior insula (not created mask)

Note: Frontal operculum (FO), rostral prefrontal cortex (RPFC), insular cortex (IC), inferior frontal gyrus (IFG)

We used the same [1 -1] to compare autistic females to TD females. We found that autistic females had greater connectivity between the right AI and various regions of the right TPJ. Autistic females displayed stronger connectivity between the right AI and the posterior division of the right MTG (2), the posterior division of the right STG, the anterior division of the right MTG, the entire right MTG, the posterior division of the left MTG, and even a bilateral mask of the MTG (Figure 3b, Table 4). All of these targets lie within the TPJ. Autistic females also had decreased connectivity between the right AI and the following regions: the posterior division of the left SMG (3a), left MFG (3b), right IFG (3a, 3b), the left IFG (3a, 3b) (Figure 3, Table 4). Furthermore, when we examined the connectivity of the left AI in autistic females, we observed both stronger and weaker connectivity to various regions in the SN and VAN compared to typically developing females. Our findings indicated that both the right and left AI have weaker connectivity patterns

to the right IFG in females with ASD (Figure 4, Table 4). We observed decreased connectivity with the left AI and the right IFG (4a), and also between the left AI and bilateral regions within the pars opercularis of the IFG (4a). We observed increased connectivity with the anterior division of the right STG (4a), anterior division of the right MTG (4b), and the posterior division of the right STG (4b) for autistic females (Figure 4, Table 5).

Figure 3: Connectivity of the right AI to the SN and VAN in females

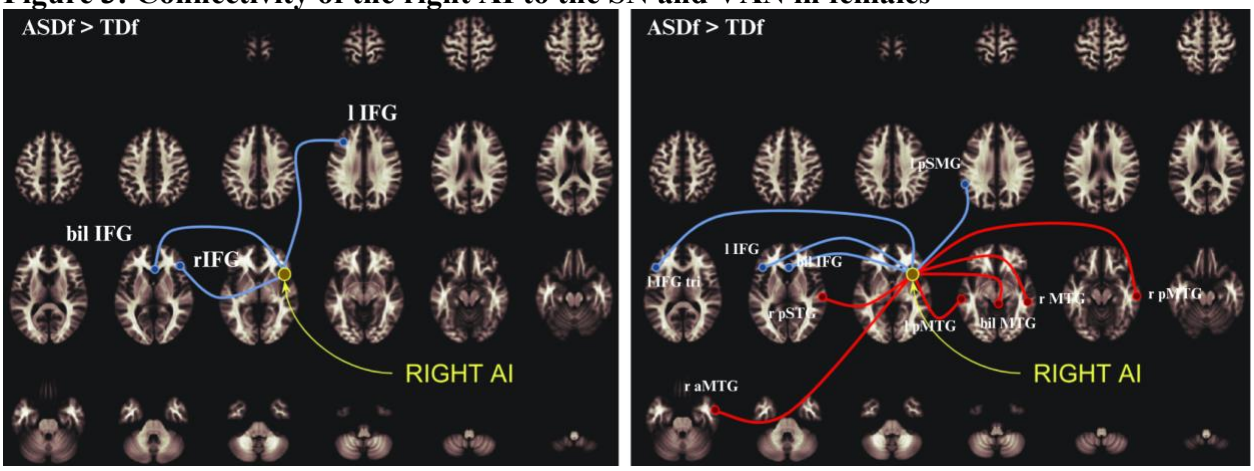

Note: Autistic female increased connectivity (ASDf > TDf) is shown in red and decreased connectivity (ASDf < TDf) is shown in blue. Significant connectivity using CONN's right AI seed centered at 47,14,0 (3a, left) and right AI mask (3b, right) as defined in Table 3.

Figure 4: Connectivity of the left AI to the SN and VAN in females

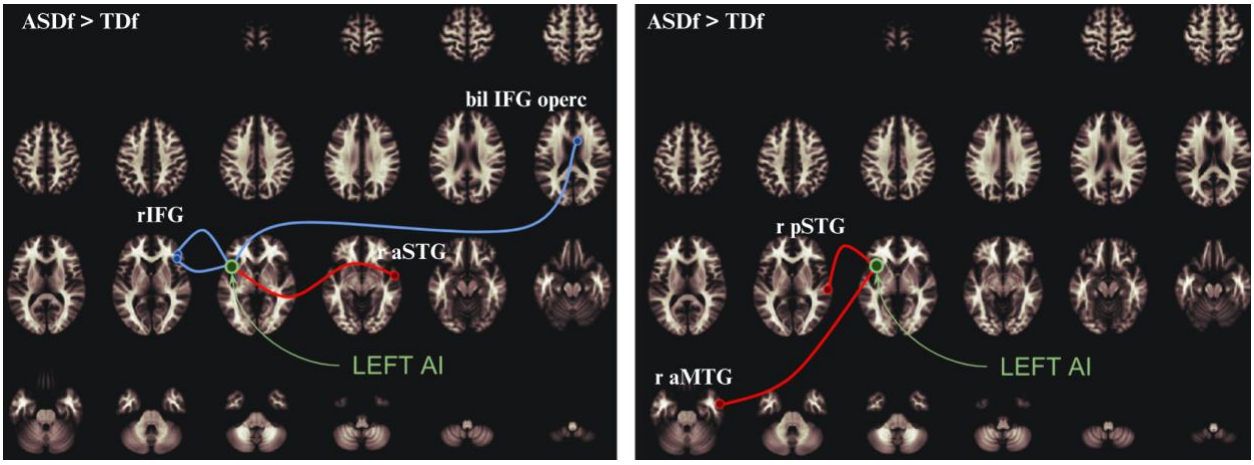

Note: Autistic female increased connectivity (ASDf > TDf) is shown in red and decreased connectivity (ASDf < TDf) is shown in blue. Connectivity from CONN's left AI seed centered at -44,13,0 (left, 4a,) and left AI mask as defined earlier (right, 4b) in Table 3.

Table 5: Summary of Results in Figures 3 and 4, altered connectivity in autistic females compared to typically developing females.

ASDf > TDf	Contrast: 1, -1				N = 20
Targets with significant differences in connectivity with the *right* AI (mask or conn's seed):					
Hyperconnectivity in ASD	beta	t-value	p-uncor.	p-FDR	Ntwk
Posterior MTG (R)	0.32	3.66	0.001783	0.169395	VAN
Posterior STG (R)	0.16	3.15	0.00555	0.263642	VAN/SN
Anterior MTG (R)	0.26	2.74	0.013521	0.369867	VAN
MTG (R)	0.23	2.67	0.015573	0.369867	VAN
Posterior MTG (L)	0.23	2.51	0.021808	0.414359	VAN
MTG (BIL)	0.23	2.3	0.033893	0.429488	VAN
Hypoconnectivity in ASD					
Whole IFG (L)	-0.21	-2.23	0.038802	0.429488	VAN
Whole IFG (BIL)	-0.2	-2.2	0.041241	0.429488	VAN
† LPFC / MFG (L)	-0.2	-2.17	0.043336	0.699616	SN
† IFG (R)	-0.21	-2.14	0.046031	0.699616	VAN
† IFG (BIL)	-0.21	-2.13	0.047473	0.699616	VAN
Posterior SMG (L)	-0.21	-2.12	0.048426	0.429488	SN
IFG pars triangularis (L)	-0.21	-2.11	0.048949	0.429488	VAN

ASDf > TDf	Contrast: 1, -1				N = 20
Targets with significant differences in connectivity with the *left* AI (mask or conn's seed):					
Hyperconnectivity in ASD	beta	t-value	p-uncor.	p-FDR	Ntwk
Anterior MTG (R)	0.21	2.76	0.012791	0.929596	VAN
Posterior STG (R)	0.15	2.48	0.023225	0.929596	VAN/SN
† Anterior STG (R)	0.2	2.32	0.032036	0.715606	VAN/SN
Hypoconnectivity in ASD					
† IFG (R)	-0.26	-2.99	0.007788	0.715606	VAN
† IFG pars opercularis (BIL)	-0.22	-2.4	0.027609	0.715606	VAN
† Whole IFG (R)	-0.21	-2.3	0.033549	0.715606	VAN

† ⇒ connectivity with conn's seed for anterior insula (not created mask)

Note: Summary of the connectivity results shown in figures 3 and 4; significant connectivity of the right or left AI to regions of the SN and VAN while using a [1, -1] contrast to compare autistic and typically developing females.

Next, we examined the impact of ASD on RSFC patterns in males and females using the [1 -1 -1 1] contrast. This contrast is derived by subtracting the female contrast from the male contrast (shown below):

$$Difference\ in\ effect\ of\ asd\ (by\ sex\ )\ =\ male\ contrast\ -\ female\ contrast$$

$$Difference\ in\ effect\ of\ asd\ (by\ sex\ )\ =\ (ASD_M\ -TD_M)\ -\ (ASD_F\ -\ TD_F)$$

$$Difference\ in\ effect\ of\ asd\ (by\ sex\ )\ =\ +ASD_M\ -TD_M\ -\ ASD_F\ +\ TD_F$$

$$Difference\ in\ effect\ of\ asd\ (by\ sex\ )\ =\ [+1\qquad -1\qquad -1\qquad +1]$$

We found that ASD caused greater decreased connectivity in males than in females, particularly within the regions that make up the TPJ. Weaker connectivity was recorded between the right AI and various regions of the MTG - posterior division of the right MTG, the posterior division of the left MTG, the anterior division of the right MTG, the entire right MTG, and a bilateral mask of the MTG - in autistic males and control females (Figure 5, Figure 6, Table 4). However, a positive beta value for the right AI's connectivity to the posterior division of the SMG suggests greater connectivity with this part of the salience network in autistic males and typical females (Figure 5, Figure 6, Table 4). Additionally, when we examined the differential effect of ASD on male connectivity versus female connectivity with the left AI, we discovered that autistic males and female controls had greater connectivity with the anterior division of the right STG (Figure 7, Figure 8, Table 4).

Figure 5: Regions whose FC with the right AI varies according to sex

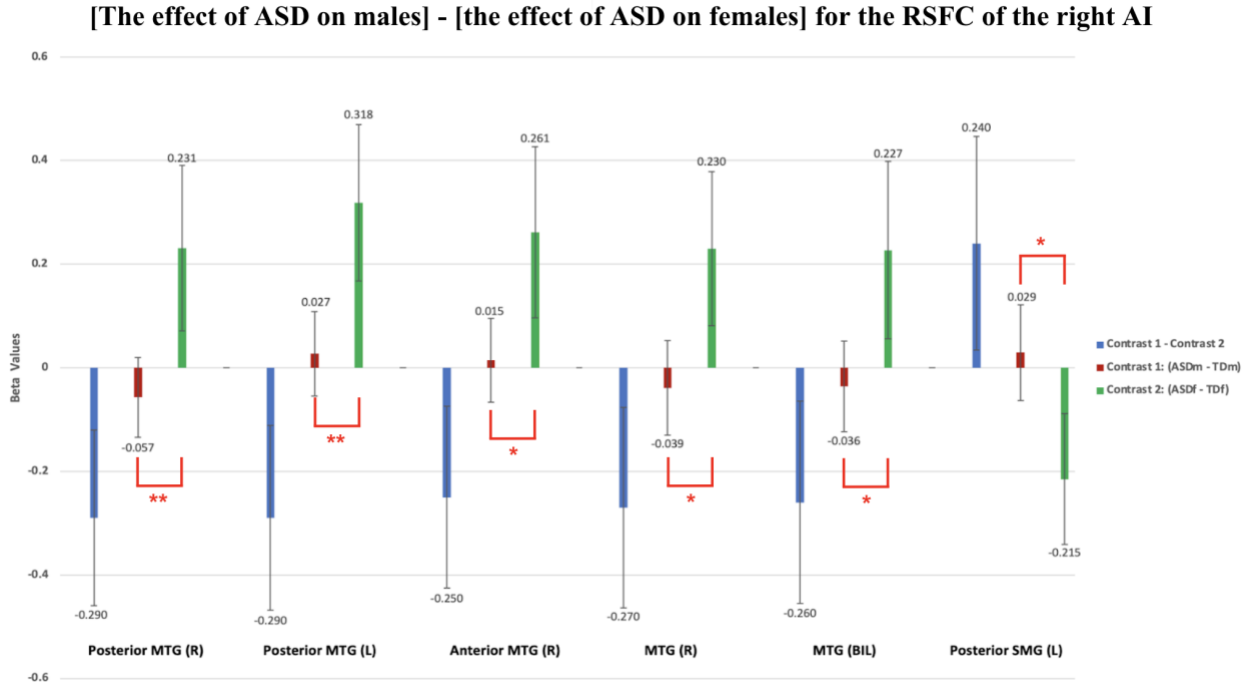

Note: Contrast 1 (red) is the [1 -1] autistic male and typical male group comparison, and Contrast 2 is the [1 -1] autistic female and typically developing female group comparison. Contrast 1 and contrast 2 are subtracted to show the difference in the effect of ASD on right AI connectivity. This difference is shown in blue and is represented by the [1 -1 -1 1] contrast. (* indicates a p-value < 0.05, ** indicates a p-value < 0.01)

Figure 6: The difference between the effect of ASD in males and females

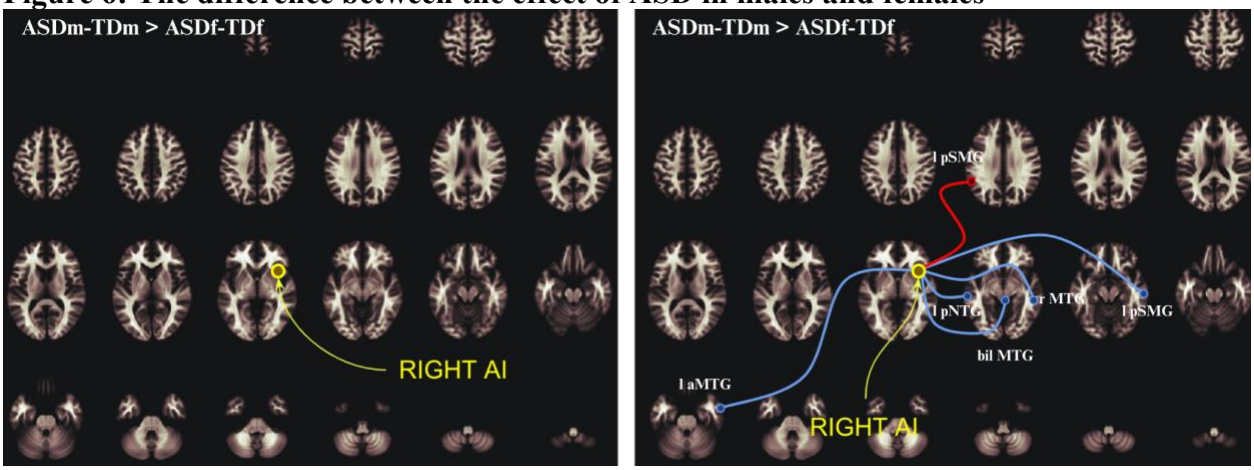

Figure 6: How ASD impacts the connectivity of males and females differentially is shown in the figure above. Increased connectivity is shown in red and decreased connectivity is shown in blue. Connectivity from CONN's right AI ROI seed centered at 47,14,0 (left, 6a,) and my left AI mask as defined earlier (right, 6b) in Table 3.

Figure 7: Difference in effect of ASD on connectivity of the left AI in each sex (graph)

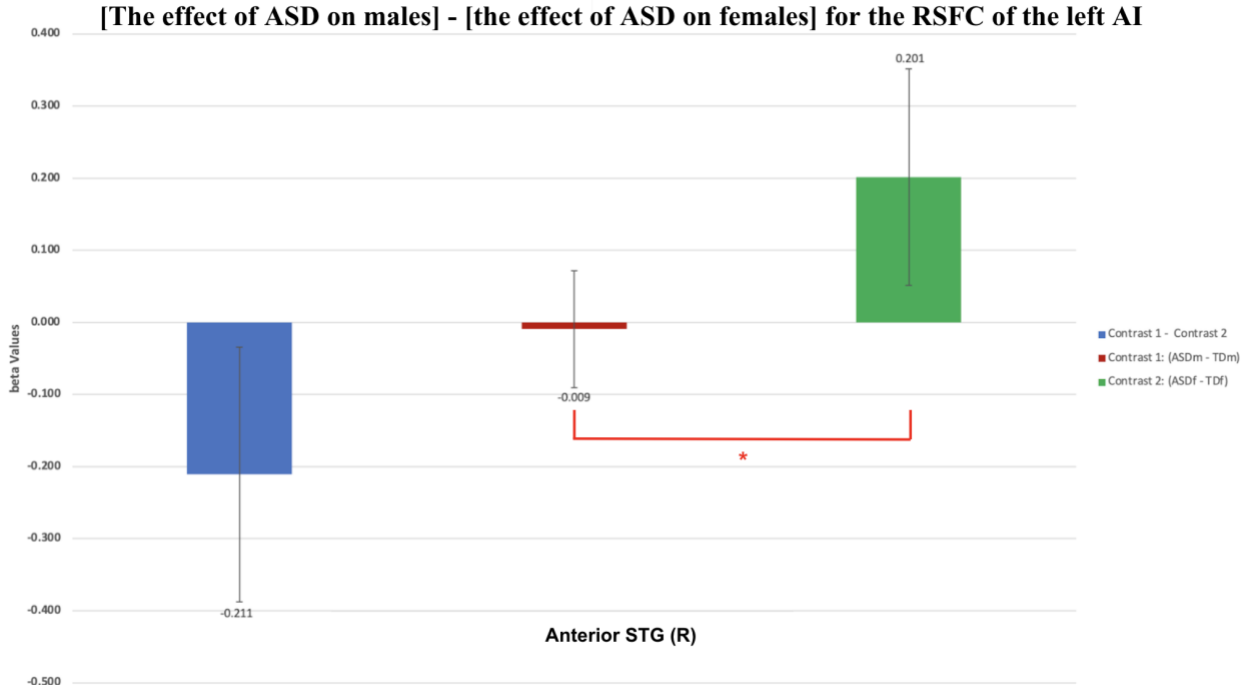

Note: Contrast 1 (red) is the [1 -1] autistic male and typical male group comparison, and Contrast 2 is the [1 -1] autistic female and typically developing female group comparison. Contrast 1 and contrast 2 are subtracted to show the difference in the effect of ASD on left AI connectivity. This difference is shown in blue and is represented by the [1 -1 -1 1] contrast. (* indicates a p-value < 0.05, ** indicates a p-value < 0.01)

Figure 8: Difference in effect of ASD on connectivity of the left AI in each sex (map)

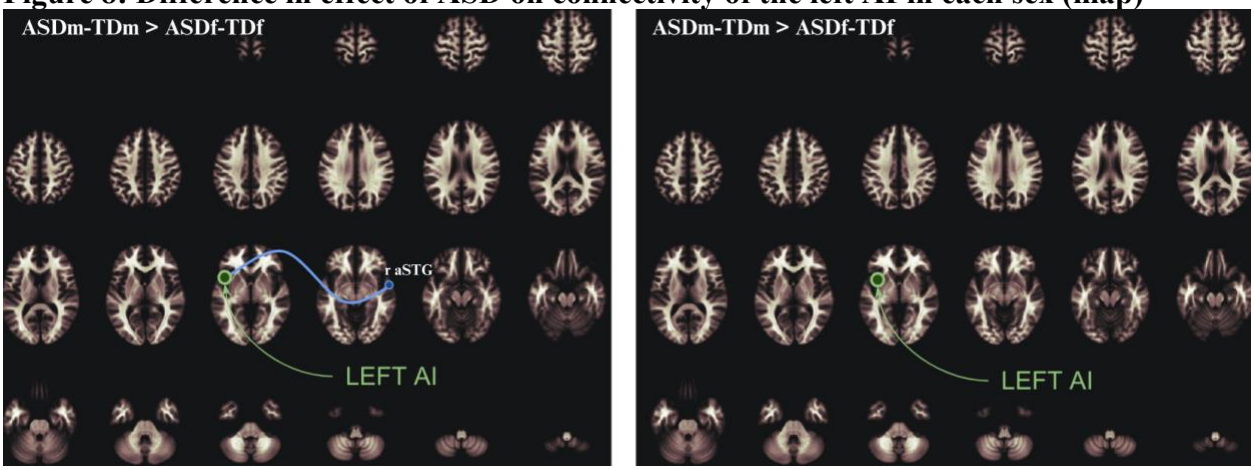

Figure 8: How ASD impacts the connectivity of males and females differentially is shown in the figure above. Increased connectivity is shown in red and decreased connectivity is shown in blue. Connectivity from CONN's left AI ROI seed centered at -44,13,0 (left, 8a,) and my left AI mask as defined earlier (right, 8b) in Table 3.

Table 6: Summary of results in Figures 5-8

$(ASD_M > TD_M) - (ASD_F > TD_F)$ Contrast: 1, -1, -1, 1 N = 92					
Targets with significant differences in connectivity with the *right* AI (mask or conn's seed):					
increased connectivity in ASD	beta	t-value	p-uncor.	p-FDR	Ntwk
Posterior SMG (L)	0.24	2.01	0.047039	0.744778	SN
Decreased connectivity in ASD					
Posterior MTG (L)	-0.29	-2.81	0.006105	0.348591	VAN
Posterior MTG (R)	-0.29	-2.74	0.007339	0.348591	VAN
Anterior MTG (R)	-0.25	-2.29	0.024444	0.484749	VAN
MTG (R)	-0.27	-2.28	0.025103	0.484749	VAN
MTG (BIL)	-0.26	-2.27	0.025513	0.484749	VAN

Lastly, we examined how the altered connectivity relates to ASD symptom scores in females and observed that an individual's connectivity value could be used to estimate SRS-2 symptom scores. For instance, for each female subject, connectivity values between the right AI and the posterior division of the left MTG were recorded because this area exhibited decreased connectivity in autistic females. A linear regression model was then applied to estimate the relationship between connectivity values and the variable of interest (SRS-2 symptom scores, SCQ scores, and ADI-R Onset Total scores). The R^2 value represents the proportion of variance in the dependent variable that is explained by the independent variable(s). In other words, determining how much of the variation in a symptom score can be predicted by the connectivity values (i.e., left AI → right pMTG). First, we looked at connectivity matrices that were significant when comparing ASD females to TD females (Figure 3, Figure 4, Table 5). Some of these matrices, such as the (1) the posterior division of the right MTG and (2) the posterior division of the right STG, can be used to accurately estimate an SRS-2 social score (Table 7, Figure 9). Additionally, some connectivity matrices to regions like the PCC were significantly correlated to SRS-2 Raw Total but did not demonstrate altered connectivity when we compared the connectivity of ASD and TD groups (Table 7, Table 5). Similarly, many of these same

regions which had altered RSFC in autistic females, as compared to female controls, were able to estimate SCQ scores and ADI-R Onset Total scores (Table 7, Figure 10, Figure 11).

Table 7: Regression model between connectivity matrices and scores

SRS

Connectivity Measure	Contrast	Source ROI -->	Target ROI	Target Ntwk	R	R2	p-value	p-value (two tailed)
1	(ASDf>TDf)	right AI	right pSTG	VAN	0.60	0.36	0.003 **	0.005 *
2	(ASDf>TDf)	right AI	right pMTG	VAN	0.58	0.34	0.003 **	0.007 **
3	(ASDf>TDf)	right AI	bilat MTG	VAN	0.52	0.27	9.9 E-04 ***	0.02 *
4	(ASDf>TDf)	right AI	left pSMG	SN	-0.42	0.18	0.03 *	0.06
5	(ASDf>TDf)	right AI	PCC	SN	0.46	0.21	0.02 *	0.043 *

SCQ

Connectivity Measure	Contrast	Source ROI -->	Target ROI	Target Ntwk	R	R2	p-value	p-value (two tailed)
1	(ASDf>TDf)	right AI	right pMTG	VAN	0.79	0.63	0.006 **	0.01 *
2	(ASDf>TDf)	right AI	† left SMG	SN	-0.75	0.57	0.009 **	0.02 *
3	(ASDf>TDf)	right AI	right aMTG	VAN	0.71	0.51	0.015 *	0.03 *
4	(ASDf>TDf)	right AI	left IFG tri	VAN	-0.64	0.41	0.03 *	0.06
5	(ASDf>TDf)	right AI	left PO	SN	-0.62	0.39	0.04 *	0.07
6	(ASDf>TDf)	right AI	left SMG	SN	-0.62	0.38	0.04 *	0.08
7	(ASDf>TDf)	right AI	right IFG	VAN	-0.59	0.35	0.03 *	0.06
8	(ASDf>TDf)	right AI	left IFG	VAN	0.53	0.28	0.049 *	0.10

ADI-Total

Connectivity Measure	Contrast	Source ROI -->	Target ROI	Target Ntwk	R	R2	p-value	p-value (two tailed)
1	(ASDf>TDf)	left AI	right aSTG	VAN	0.71	0.5	0.038 *	0.076
2	(ASDf>TDf)	right AI	left pSMG	SN	0.82	0.68	0.011 *	0.023 *
3	(ASDf>TDf)	right AI	right aSMG	SN	0.85	0.73	0.007 **	0.014 *
4	(ASDf>TDf)	right AI	† right SMG	SN	0.74	0.55	0.029 *	0.06
5	(ASDf>TDf)	right AI	right SMG	SN	0.84	0.71	0.009 **	0.018 *

† means CONN's ROI when the connectivity matrices of both CONN's ROI and my ROI correlated significantly with a given assessment score

Note: (7a) Correlations to the SRS-2 Raw Total scores, SCQ scores, and ADI-R Onset Total scores via a linear regression model. (* indicates a p-value < 0.05, ** indicates a p-value < 0.01, *** indicates a p-value < 0.001).

Figure 9: SRS-2 Regression for (right AI → pSTG) connectivity matrix

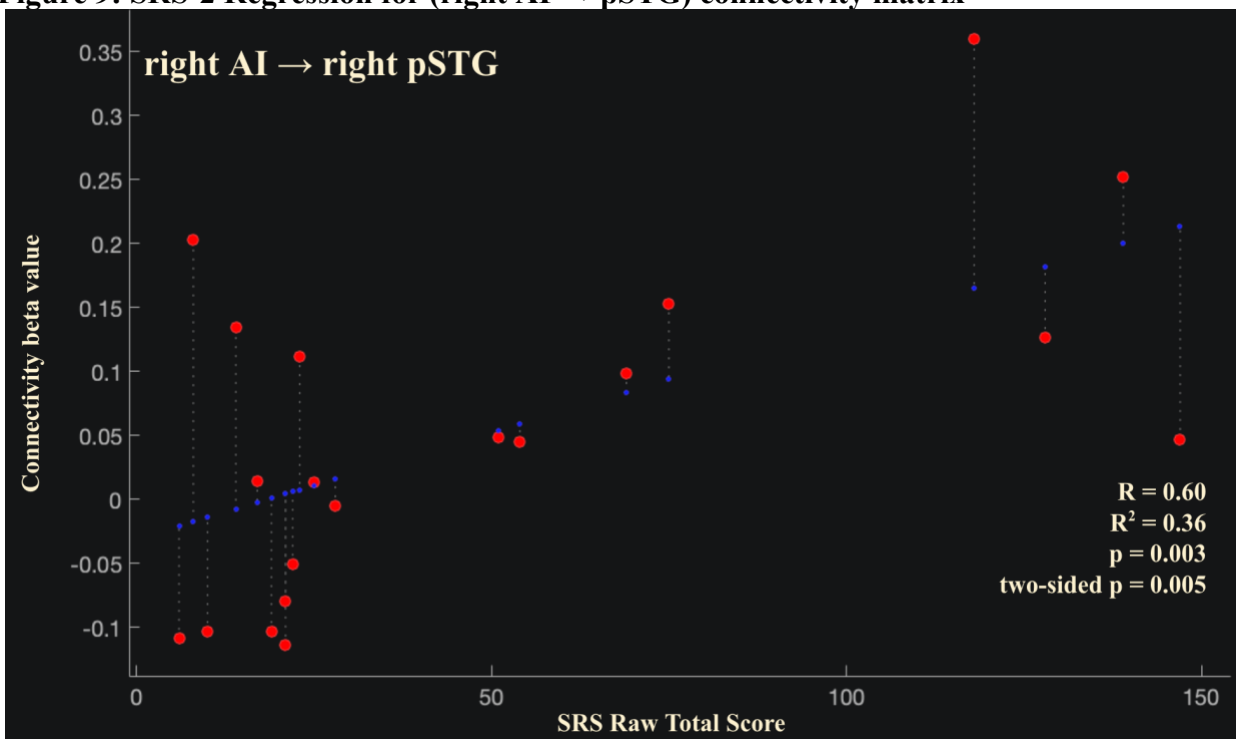

Note: N=20, Red dots are observed values and blue dots are fitted values. The Y-axis is connectivity values, and the x-axis is the ADI-R Onset Total scores.

Figure 10: SCQ Regression for (right AI → right pMTG) connectivity matrix

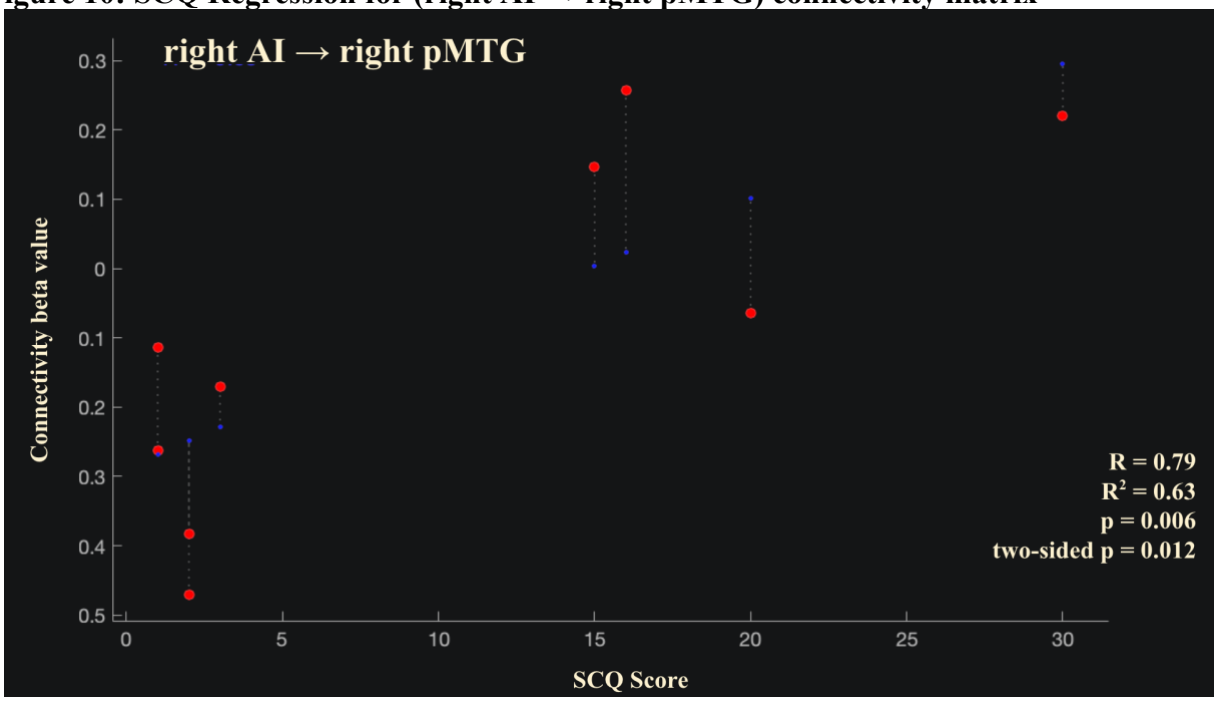

Note: N=10, Red dots are observed values and blue dots are fitted values. The Y-axis is connectivity values, and the x-axis is the ADI-R Onset Total scores.

Figure 11: ADI-R Onset Total Score Regression for (right AI → right aSMG) connectivity matrix

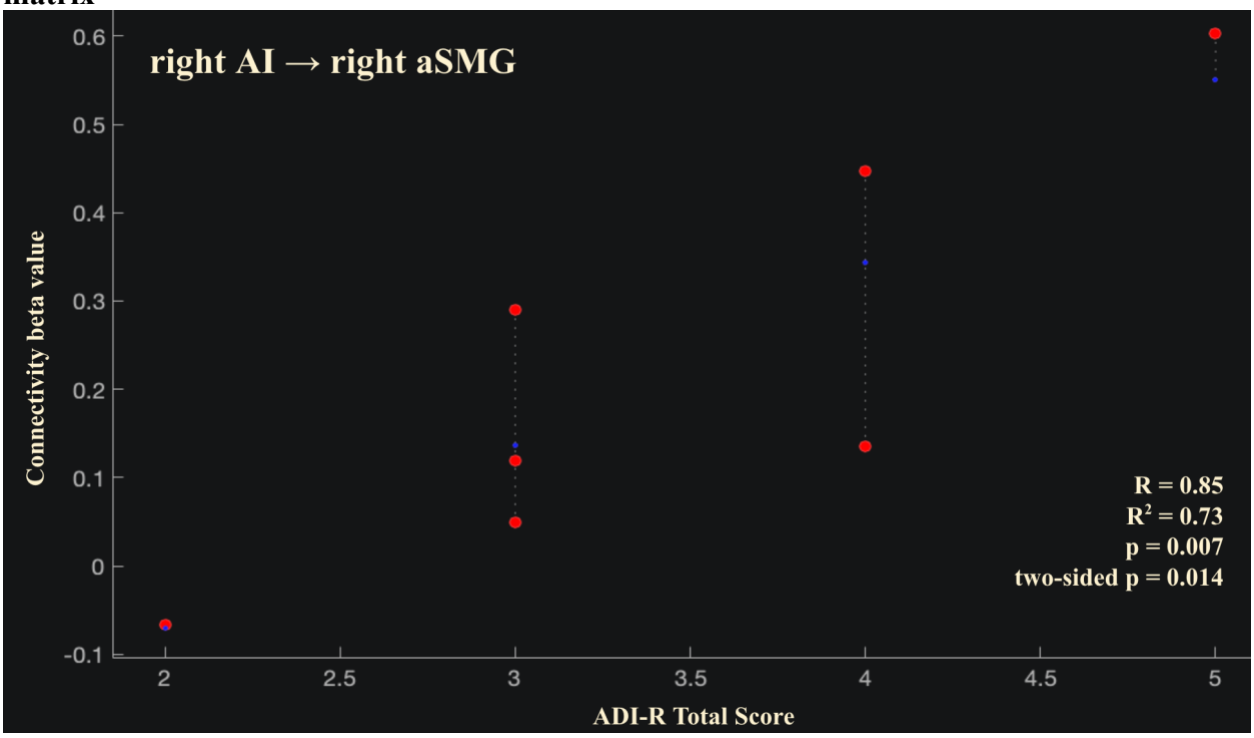

Note: N=8, Red dots are observed values and blue dots are fitted values. The Y-axis is connectivity values, and the x-axis is the ADI-R Onset Total scores.

Discussion

In this study, we aimed to investigate the RSFC patterns of the SN and VAN in children aged 8-12 years old with and without autism spectrum disorder (ASD). We used a ROI-based approach to analyze the RSFC patterns of the AI and targets in the SN and VAN. Our findings suggest that there are significant differences in RSFC between children with and without ASD. We found decreased connectivity in the SN - specifically between the left AI and the right IFG in autistic males compared to TD males and also between the right AI and right IFG in autistic females compared to TD females. Moreover, in autistic females but not autistic males, we found increased connectivity in the VAN between the AIs on both hemispheres and the right TPJ - including the MTG and STG - relative to TD females. Perhaps, this reflects a compensatory

mechanism in autistic males. However, our findings did not support our hypothesis of increased connectivity between the AI and the SN in autistic females, and the increased connectivity in the VAN was limited to regions that make up the TPJ. These results built upon past findings that there are significant differences in RSFC patterns between children with ASD and TD children in the SN and VAN (von dem Hagen et al., 2012).

It is interesting that the SCQ score average for typically developing males (mean = 4.33) is significantly larger than the average for typically developing females (mean = 1.80) (Table 1). We observed a p-value of 0.03 for this sex-difference. Conversely, an insignificant ($p = 0.18$) but potentially related trend showed that autistic females (mean = 20.25) had a higher SCQ score than autistic males (mean =15.33) (Table 1). Although even less significant, most other assessments (i.e., the FIQ, VIQ, ADI-R Social, ADI-Verbal, ADI-R RRB, and the SRS Total) also demonstrated this trend where autistic females had larger scores for ASD symptoms or severity (Table 1). This may reflect a bias within the SCQ assessment for male-like traits or behaviors, which may relate to the increase in diagnostic follow-ups for autism and the increased prevalence of autism in males. In other words, females may be diagnosed less frequently due to a diagnostic preference for male-like traits in screening assessment like the SCQ. This may lead to autistic females exhibiting more severe scores for autism on other metrics once individuals pass the threshold for further examination on screening assessments like the SCQ. This would also be supported by our data which showed that the effect of autism on RSFC in autistic females, which was larger in terms of magnitude and number of differences. Alternatively, these data may provide further evidence for the social “masking” or “camouflaging” in autistic females, which has led to lower screening scores in females and attributed to the difference in the prevalence of autism in each sex (Rynkiewicz et al., 2016; Schuck et al., 2019).

In addition to our expectations to observe AI connectivity differences between the sexes, our study also produced some unexpected results. Specifically, we did not find evidence of increased connectivity between the AI and the SN in male children with ASD, as we had hypothesized. Although contrary to our hypotheses, our results are still consistent with other previous studies which have reported decreased connectivity in this network in individuals with ASD (Francis et al., 2019; Odriozola et al., 2015). There are many potential explanations for this discrepancy including age, between-scanner effects, the heterogeneity of autism, sample size, etc. (Spreng et al., 2016; Carp, J., 2012). It is possible that increased connectivity in the SN network is more prominent in individuals with ASD who are at different stages of development.

Our final [1 -1 -1 1] contrast highlighted how ASD impacts each sex differently. These results suggest that there may be sex-dependent effects of autism on connectivity within the VAN and SN, which is a novel finding in the field. One explanation for the inconsistency in male and female connectivity is that female brains are more developed during the eight to twelve years of age (Cole et al., 2008; Sanders et al., 2023), the age range of this study. The greater maturation of female brains is one possible explanation for the striking difference between males and females with autism. Some studies have even reported that regions of the brain which are also associated with emotional processing and empathy, tend to have stronger connectivity in autistic females than males between the ages of seven and thirteen (Smith et al., 2019). Although some studies have found both hypoconnectivity and hyperconnectivity (Uddin et al., 2013), some have pointed to maturational changes to explain these inconsistencies in ASD (Xu et al., 2018). Thus, our results may reflect a developmental sex difference in brain trajectory for autistic individuals. A longitudinal study on the FC of the AI within the SN and VAN with a greater number of subjects would provide greater clarity on this matter.

Additionally, the final [1 -1 -1 1] contrast brought to light some interesting points. This contrast is the difference between the two earlier contrasts where we compared ASD and TD subjects for each sex independently. Therefore, the regions that displayed significant connectivity alterations represent regions that are affected by ASD differently based on sex. Therefore, it is interesting that five of the six significant ROIs were part of the TPJ and therefore VAN, and each of these five regions demonstrated the same effect. One way to interpret this is that the effect of ASD in females for these regions is a much larger increase in connectivity compared to sex-matched controls. This may relate to the theory of mind (ToM), which is the ability to attribute mental states like beliefs, intentions, and desires to oneself and others. ToM is important in social cognition and critical for successful social interactions (Xu et al., 2015). The greater connectivity to ToM and TPJ structures autistic females (compared to autistic males) may contribute to greater social skills. Moreover, of these five VAN targets where females seemed to have greater connectivity, only one was on the left hemisphere (posterior division of the left MTG), which may relate to the finding that the VAN is predominantly controlled by the right hemisphere (Downar et al., 2020).

Conversely, the sixth significant ROI in this contrast, the left SMG, is part of the SN, not the VAN. This region had an opposite effect where the effect of ASD in females was more pronounced again, but in the opposite direction (a much larger decrease in connectivity) compared to sex-matched controls. This finding is very interesting because it relates to our next discovery. When we correlated connectivity to the SRS-2 Raw Total scores, the (right AI → left SMG) connectivity values were the only ones with a significant negative correlation with SRS-2 scores that also displayed altered connectivity in autistic females (compared to TD females in Table 3

and Figures 3-4, Figure 6). Together, these findings raise questions about the SMG's role across sex.

The greater prevalence of autism in males could be due to several factors, such as sex-specific differences in brain development or socialization. Research has shown that females with ASD may exhibit different behavioral characteristics compared to males, such as higher levels of social communication abilities and better adaptive skills. It is possible that our observed differences in connectivity when using the [1 -1 -1 1] contrast may relate to these behavioral differences. The regions with significant differences in connectivity for this contrast were the right MTG, left MTG and left SMG, right STG. The MTG is associated with social cognition, semantic processing, and theory of mind (Xu et al., 2015) which is known to be compromised in autism (Yu et al., 2020). SMG is associated with language comprehension, visuospatial processing, and empathy (Deschamps et al., 2014; Ben-Shabat et al., 2015; Zhao et al., 2021). The STG is associated with auditory processing, and social perception (Pelphrey et al., 2004; McAlonan et al., 2005). These regions have been previously implicated in the development of ASD (Salmi et al., 2013; Zhao et al., 2021; McAlonan et al., 2015).

Furthermore, the increased connectivity in the VAN observed in autistic females compared to males (Figures 5-8, Table 6) may have explanatory value in the differences in social cognition deficits between autistic males and females (Mattern et al., 2023). On the other hand, the reduced connectivity between the right AI and left SMG in autistic males may underlie some of the behavioral differences observed between autistic males and females. Techniques like TMS and neurofeedback have been used to alter the RSFC between regions of the brain before (Tang et al., 2021; Ramot et al., 2017). Our findings may have implications for developing targeted interventions for individuals with ASD, again, raising the importance of researching the targets of

this study independently by sex as candidates for improving salience and social cognition in autistic children.

Lastly, our preliminary results correlating connectivity with symptom scores highlight the usefulness of our methods in predicting symptom scores with ASD. In addition to connectivity values between the right or left AI and regions of the TPJ and the SMG, connectivity with other regions which were not statistically significant in ASD-TD comparisons, such as the PCC and PO, proved useful in our estimations of SRS-2, SCQ, and ADI-R Onset Total scores (Table 7). However, it is important to note that our calculations assumed a linear relationship between connectivity values and the variable of interest. With nonlinear relationships, the R^2 value may not accurately reflect the strength of the association (Rose & McGuire, 2019). Nevertheless, our findings highlight the potential for the RSFC of VAN structures to be a useful biomarker for symptomology in ASD and suggest the need for future investigation in this area.

It is important to note that our study was limited in that we only included children who were able to complete the scan, which may have limited the generalizability of our results to individuals with more severe forms of ASD. Another important limitation is the lack of significant FDR-corrected (FDR = false discovery rate) p-values (Nickerson, 2018; Vul et al., 2009), potentially reducing the reproducibility of our results. However, in reality, because we included so many superfluous ROIs our data is not conducive to yielding any significant FDR-corrected p values. After restructuring our ROIs, we would have significant p-values after an FDR correction. Despite these limitations, our findings have important implications for understanding the neural underpinnings of ASD. Specifically, our results suggest that there may be sex-dependent effects of ASD on connectivity within the SN and VAN, which may contribute to the variability of ASD symptoms observed in males and females. Additionally, the potential sex-dependent effects of

ASD on connectivity within the SN and VAN that we observed is particularly relevant to the fact that autism is diagnosed more frequently in males than in females.

Conclusion

In conclusion, our study provides novel insights into the functional connectivity patterns of the SN and VAN in children with and without ASD. Our results suggest that there are significant differences in connectivity between these networks in children with ASD, particularly in the regions of the TPJ and SMG. Additionally, our findings highlight the importance of considering sex differences in the neural mechanisms of ASD. Our preliminary results correlating connectivity provide an example of how resting-state connectivity between the AI and VAN regions could be used in the future with advances in technology and medicine to gain information about a patient's behavioral symptoms before an assessment is even given. Overall, our study contributes to a growing body of literature on the neural underpinnings of ASD and may inform the development of more targeted interventions for individuals with this disorder.

Supplemental Information

Detailed Preprocessing:

We modeled our preprocessing of functional and anatomical data using a CONN's default pipeline (Nieto-Castanon, 2020) and created a MATLAB script to automate the preprocessing for each subject to ensure no errors were made as subjects were added. First, we corrected for motion and magnetic susceptibility interactions by realigning the functional data using a least squares

approach and a 6-parameter transformation (Friston et al., 1996). Next, we corrected for temporal misalignment between different slices, or slice timing correction, of the functional data using sinc temporal interpolation (Sladky et al., 2011). We identified outlier scans using ART (9) and computed a reference BOLD image for each subject by averaging all scans excluding outliers. Outliers were identified as acquisitions with framewise displacement over 0.9 mm or global BOLD signal changes above 5 standard deviations (Power et al., 2014), and a reference BOLD image was computed for each subject by averaging all scans excluding outliers. We normalized the functional and anatomical data into standard MNI space and segmented them into grey matter, white matter, and CSF tissue classes and were resampled to 2 mm isotropic voxels (2 mm x 2 mm x 2 mm) following a direct normalization procedure using the SPM unified segmentation and normalization algorithm (Ashburner and Friston, 2005; Ashburner, 2007) with the IXI-549 tissue probability map template which is commonly used in pediatric fMRI studies (Cummings et al., 2020). Last, functional data were smoothed using spatial convolution with a Gaussian kernel of 8 mm full width half maximum (FWHM).

Bibliography

Alaerts K, Swinnen SP, Wenderoth N (2016) Sex differences in autism: A resting-state fmri investigation of functional brain connectivity in males and females. Social Cognitive and Affective Neuroscience 11:1002–1016.

Allen M, Fardo F, Dietz MJ, Hillebrandt H, Friston KJ, Rees G, Roepstorff A (2016) Anterior insula coordinates hierarchical processing of tactile mismatch responses. NeuroImage 127:34–43.

Anderson JS, Nielsen JA, Froehlich AL, DuBray MB, Druzgal TJ, Cariello AN, Cooperrider JR, Zielinski BA, Ravichandran C, Fletcher PT, Alexander AL, Bigler ED, Lange N, Lainhart JE (2011) Functional Connectivity Magnetic Resonance Imaging Classification of Autism. Brain 134:3742–3754.

Ashburner J (2007) A fast diffeomorphic image registration algorithm. NeuroImage 38:95–113.

Ashburner J, Friston KJ (2005) Unified segmentation. NeuroImage 26:839–851.

Baron-Cohen S, Ashwin E, Ashwin C, Tavassoli T, Chakrabarti B (2009) Talent in autism: Hyper-systemizing, hyper-attention to detail and sensory hypersensitivity. Philosophical Transactions of the Royal Society B: Biological Sciences 364:1377–1383.

Ben-Shabat E, Matyas TA, Pell GS, Brodtmann A, Carey LM (2015) The right supramarginal gyrus is important for proprioception in healthy and stroke-affected participants: A functional MRI study. Frontiers in Neurology 6.

Benjamini Y, Hochberg Y (1995) Controlling the false discovery rate: A practical and powerful approach to multiple testing. Journal of the Royal Statistical Society: Series B (Methodological) 57:289–300.

Berument SK, Rutter M, Lord C, Pickles A, Bailey A (1999) Autism screening questionnaire: Diagnostic validity. British Journal of Psychiatry 175:444–451.

Bishop-Fitzpatrick L, Mazefsky C, Eack S, Minshew N (2017) Correlates of social functioning in autism spectrum disorder: The role of social cognition. Research In Autism Spectrum Disorders, 35, 25-34.

Bonnelle V, Ham TE, Leech R, Kinnunen KM, Mehta MA, Greenwood RJ, Sharp DJ (2012) Salience network integrity predicts default mode network function after traumatic brain injury. Proceedings of the National Academy of Sciences 109:4690–4695.

Cole WR, Mostofsky SH, Larson JC, Denckla MB, Mahone EM (2008) Age-related changes in motor subtle signs among girls and boys with ADHD. Neurology 71:1514–1520.

Caria A, de Falco S (2015) Anterior insular cortex regulation in autism spectrum disorders. Frontiers in Behavioral Neuroscience 9.

Chan W, Smith L, Hong J, Greenberg J, Mailick M (2017) Validating the social responsiveness scale for adults with autism. Autism Research, 10(10), 1663-1671.

Cummings KK, Lawrence KE, Hernandez LM, Wood ET, Bookheimer SY, Dapretto M, Green SA (2020) Sex differences in salience network connectivity and its relationship to sensory over-responsivity in youth with autism spectrum disorder. Autism Research 13:1489–1500.Breslin P (2013) An evolutionary perspective on food and human taste. Current Biology, 23(9), 409–418.

Deschamps I, Baum SR, Gracco VL (2014) On the role of the supramarginal gyrus in phonological processing and verbal working memory: Evidence from RTMS studies. Neuropsychologia 53:39–46.

Dougherty JD, Marrus N, Maloney SE, Yip B, Sandin S, Turner TN, Selmanovic D, Kroll KL, Gutmann DH, Constantino JN, Weiss LA (2022) Can the “Female protective effect” liability threshold model explain sex differences in autism spectrum disorder? Neuron 110:3243–3262.

Downar J, Crawley A, Mikulis D, Davis K (2000) A multimodal cortical network for the detection of changes in the sensory environment. *Nature Neuroscience*, *3*(3), 277–283.

Farrant K, Uddin LQ (2015) Atypical development of dorsal and ventral attention networks in autism. Developmental Science 19:550–563.

Fitzgerald J, Johnson K, Kehoe E, Bokde A, Garavan H, Gallagher L, McGrath J (2014) Disrupted Functional Connectivity in Dorsal and Ventral Attention Networks During Attention Orienting in Autism Spectrum Disorders. Autism Research, 8(2), 136-152.

Francis SM, Camchong J, Brickman L, Goelkel-Garcia L, Mueller BA, Tseng A, Lim KO, Jacob S (2019) Hypoconnectivity of insular resting-state networks in adolescents with autism spectrum disorder. Psychiatry Research: Neuroimaging 283:104–112.

Friston KJ, Williams S, Howard R, Frackowiak RS, Turner R (1996) Movement-related effects in fmri time-series. Magnetic Resonance in Medicine 35:346–355.

Gotham K, Risi S, Pickles A, Lord C (2006) The Autism Diagnostic Observation Schedule: Revised Algorithms for Improved Diagnostic Validity. Journal Of Autism And Developmental Disorders, 37(4), 613-627.

Gotham K, Pickles A, Lord C (2008) Standardizing ADOS™-2 Scores for a Measure of Severity in Autism Spectrum Disorders. Journal Of Autism And Developmental Disorders, 39(5), 693-705.

Guo X, Duan X, Suckling J, Chen H, Liao W, Cui Q, Chen H (2018) Partially impaired functional connectivity states between right anterior insula and default mode network in autism spectrum disorder. Human Brain Mapping, 40(4), 1264-1275.

Hallquist MN, Hwang K, Luna B (2013) The nuisance of nuisance regression: Spectral misspecification in a common approach to resting-state fmri preprocessing reintroduces noise and obscures functional connectivity. NeuroImage 82:208–225.

Hull JV, Dokovna LB, Jacokes ZJ, Torgerson CM, Irimia A, Van Horn JD (2017) Resting-state functional connectivity in autism spectrum disorders: A Review. Frontiers in Psychiatry 7.

Iuculano T, Padmanabhan A, Chen L, Nicholas J, Mitsven S, de los Angeles C, Menon V (2020) Neural correlates of cognitive variability in childhood autism and relation to heterogeneity in decision-making dynamics. Developmental Cognitive Neuroscience 42:100754.

Jung M, Tu Y, Park J, Jorgenson K, Lang C, Song W, Kong J (2018) Surface-based shared and distinct resting functional connectivity in attention-deficit hyperactivity disorder and autism spectrum disorder. The British Journal Of Psychiatry, 214(06), 339-344.

Klugah-Brown B, Wang P, Jiang Y, Becker B, Hu P, Biswal B (2021) Structural-functional connectivity mapping of the insular cortex system: A combined data-driven and meta-analytic topic mapping approach, bioRxiv.

Lai M-C, Lombardo MV, Ruigrok ANV, Chakrabarti B, Auyeung B, Szatmari P, Happé F, Baron-Cohen S (2016) Quantifying and exploring camouflaging in men and women with autism. Autism 21:690–702.

Lancaster JL, Rainey LH, Summerlin JL, Freitas CS, Fox PT, Evans AC, Toga AW, Mazziotta JC (1997) Automated labeling of the human brain: A preliminary report on the development and evaluation of a forward-transform method. Human Brain Mapping 5:238–242.

Lawrence K, Abaryan Z, Laltoo E, Hernandez L, Gandal M, McCracken J, Thompson M (2022) White matter microstructure shows sex differences in late childhood: Evidence from 6797 children. *Human Brain Mapping*.

Lawrence K, Hernandez LM, Bowman HC, Padgaonkar NT, Fuster E, Jack A, Aylward E, Gaab N, Van Horn JD, Bernier RA, Geschwind DH, McPartland JC, Nelson CA, Webb SJ, Pelphrey KA, Green SA, Bookheimer SY, Dapretto M (2020) Sex differences in

functional connectivity of the salience, default mode, and Central Executive Networks in youth with ASD. Cerebral Cortex 30:5107–5120.

Leekam SR, Prior MR, Uljarevic M (2011) Restricted and repetitive behaviors in autism spectrum disorders: A review of research in the last decade. Psychological Bulletin 137:562–593.

Loomba N, Beckerson M, Ammons C, Maximo J, Kana R, (2021) Corpus callosum size and homotopic connectivity in Autism spectrum disorder.

Psychiatry Research: Neuroimaging, 313, 111301.

Maldjian JA, Laurienti PJ, Kraft RA, Burdette JH (2003) An automated method for neuroanatomic and cytoarchitectonic Atlas-based interrogation of fmri data sets. NeuroImage 19:1233–1239.

Mattern H, Cola M, Tena KG, Knox A, Russell A, Pelella MR, Hauptmann A, Covello M, Parish-Morris J, McCleery JP (2023) Sex differences in social and emotional insight in youth with and without autism. Molecular Autism 14.

McAlonan GM, Cheung V, Cheung C, Suckling, J Lam, GY Tai KS, Chua SE (2005) Mapping the brain in autism. A voxel-based MRI study of volumetric differences and intercorrelations in autism. Brain, 128(2), 268-276. say about the STG

Menon V, Cerri D, Lee B, Yuan R, Lee S-H, Shih Y-YI (2022) Optogenetic stimulation of anterior insular cortex neurons reveals causal mechanisms underlying suppression of the default mode network by the Salience Network.

Nickerson LD (2018) Replication of resting state-task network correspondence and novel findings on Brain Network activation during task fmri in the Human Connectome Project Study. Scientific Reports 8.

Nieto-Castanon A (2020) FMRI denoising pipeline. Handbook of functional connectivity Magnetic Resonance Imaging methods in CONN:17–25.

Nieto-Castanon A (2020) General linear model. Handbook of functional connectivity Magnetic Resonance Imaging methods in CONN:63–82.

Nieto-Castanon A (2020) FMRI minimal preprocessing pipeline. In *Handbook of functional connectivity Magnetic Resonance Imaging methods in CONN* (pp. 3–16). Hilbert Press. doi:10.56441/hilbertpress.2207.6599

Nieto-Castanon A (2020) Preparing fMRI Data for Statistical Analysis. In M. Filippi (Ed.). fMRI techniques and protocols. Springer. doi:10.48550/arXiv.2210.13564

Odriozola P, Uddin LQ, Lynch CJ, Kochalka J, Chen T, Menon V (2015) Insula response and connectivity during social and non-social attention in children with autism. Social Cognitive and Affective Neuroscience 11:433–444.

Onofrj V, Chiarelli A, Wise R, Colosimo C, Caulo M (2022) Interaction of the salience network, ventral attention network, dorsal attention network and default mode network in neonates and early development of the bottom-up attention system. *Brain Structure and Function*, *227*(5), 1843–1856.

Pelphrey KA, Morris JP, McCarthy G (2004) Grasping the intentions of others: the perceived intentionality of an action influences activity in the superior temporal sulcus during social perception. Journal of Cognitive Neuroscience, 16(10), 1706-1716.

Power JD, Mitra A, Laumann TO, Snyder AZ, Schlaggar BL, Petersen SE (2014) Methods to detect, characterize, and remove motion artifacts in resting state fmri. NeuroImage 84:320–341.

Power JD, Barnes KA, Snyder AZ, Schlaggar BL, Petersen SE (2017) Spurious but systematic correlations in functional connectivity MRI networks arise from subject motion. NeuroImage, 153, 214-230.

Prokopiou PC, Kassinopoulos M, Xifra-Porxas A, Boudrias M-H, Mitsis GD (2020) Modeling the hemodynamic response function using simultaneous EEG-fmri data and convolutional sparse coding analysis with RANK-1 constraints. bioRxiv Available at: https://www.biorxiv.org/content/10.1101/2020.09.09.290296v1.full [Accessed March 25, 2023].

Pua EP, Thomson P, Yang JY-M, Craig JM, Ball G, Seal M (2020) Individual differences in intrinsic brain networks predict symptom severity in autism spectrum disorders. Cerebral Cortex 31:681–693.

Ramot M, Kimmich S, Gonzalez-Castillo J, Roopchansingh V, Popal H, White E, Gotts SJ, Martin A (2017) Direct modulation of Aberrant Brain Network connectivity through real-time neurofeedback. eLife 6.

Reis H, Eusébio I, Sousa M, Ferreira M, Pereira R, Dias S, Reis CI (2021) Regul-A: A technological application for sensory regulation of children with autism spectrum disorder in the home context. International Journal of Environmental Research and Public Health 18:10452.

Rose S, McGuire TG (2019) Limitations of *p*-values and *r*-squared for stepwise regression building: A fairness demonstration in Health Policy Risk Adjustment. The American Statistician 73:152–156.

Rynkiewicz A, Schuller B, Marchi E, Piana S, Camurri A, Lassalle A, Baron-Cohen S (2016) An investigation of the 'female camouflage effect' in autism using a computerized ADOS-2 and a test of sex/gender differences. Molecular Autism 7.

Saad ZS, Gotts SJ, Murphy K, Chen G, Jo HJ, Martin A, Cox RW (2012) Trouble at rest: How correlation patterns and group differences become distorted after global signal regression. Brain Connectivity 2:25–32.

Salmi J, Roine U, Glerean E, Lahnakoski J, Nieminen-von Wendt T, Tani P, Leppämäki S, Nummenmaa L, Jääskeläinen IP, Carlson S, Rintahaka P, Sams M (2013) The brains of high functioning autistic individuals do not synchronize with those of others. NeuroImage: Clinical 3:489–497.

Sanders AF, Harms MP, Kandala S, Marek S, Somerville LH, Bookheimer SY, Dapretto M, Thomas KM, Van Essen DC, Yacoub E, Barch DM (2023) Age-related differences in resting-state functional connectivity from childhood to adolescence. Cerebral Cortex.

Schuck RK, Flores RE, Fung LK (2019) Brief report: Sex/gender differences in symptomology and camouflaging in adults with autism spectrum disorder. Journal of Autism and Developmental Disorders 49:2597–2604.

Shaw KA et al. (2023) Early identification of autism spectrum disorder among children aged 4 years — autism and Developmental Disabilities Monitoring Network, 11 sites, United States, 2020. MMWR Surveillance Summaries 72:1–15.

Sladky R, Friston KJ, Tröstl J, Cunnington R, Moser E, Windischberger C (2011) Slice-timing effects and their correction in functional MRI. NeuroImage 58:588–594.

Smith RE, Avery JA, Wallace GL, Kenworthy L, Gotts SJ, Martin A (2019) Sex differences in resting-state functional connectivity of the cerebellum in autism spectrum disorder. Frontiers in Human Neuroscience 13.

Spreng, RN, Stevens, WD, Viviano, JD, Schacter, DL (2016) Attenuated anticorrelation between the default and dorsal attention networks with aging: evidence from task and rest. Neurobiology of aging, 45, 149-160.

Tang N, Sun C, Wang Y, Li X, Liu J, Chen Y, Sun L, Rao Y, Li S, Qi S, Wang H (2021) Clinical response of major depressive disorder patients with suicidal ideation to individual target-transcranial magnetic stimulation. Frontiers in Psychiatry 12.

Tavares V, Fernandes LA, Antunes M *et al.* Sex Differences in Functional Connectivity Between Resting State Brain Networks in Autism Spectrum Disorder. *J Autism Dev Disord* 52, 3088–3101 (2021).

Touroutoglou A, Bliss-Moreau E, Zhang J, Mantini D, Vanduffel W, Dickerson B, Barrett L (2016) A ventral salience network in the macaque brain. Neuroimage, 132, 190-197.

Uddin L, Supekar K, Lynch C, Khouzam A, Phillips J, Feinstein C, Ryali S, Menon V (2013) Salience network–based classification and prediction of symptom severity in children with autism. *JAMA Psychiatry*, *70*(8), 869.

Uddin LQ, Menon V (2009) The anterior insula in autism: Under-connected and under-examined. Neuroscience Biobehavioral Reviews 33:1198–1203.

Van Dijk KRA, Sabuncu MR, Buckner RL (2012) The influence of head motion on intrinsic functional connectivity MRI. NeuroImage 59:431–438.

Vul E, Harris C, Winkielman P, Pashler H (2009) Puzzlingly high correlations in fmri studies of emotion, personality, and social cognition. Perspectives on Psychological Science 4:274–290.

von dem Hagen E, Stoyanova R, Baron-Cohen S, Calder A (2012) Reduced functional connectivity within and between 'social' resting state networks in autism spectrum conditions. *Social Cognitive and Affective Neuroscience*, *8*(6), 694–701.

Xu J, Wang H, Zhang L, Xu Z, Li T, Zhou Z, Zhou Z, Gan Y, Hu Q (2018) Both hypo-connectivity and hyper-connectivity of the insular subregions associated with severity in children with autism spectrum disorders. Frontiers in Neuroscience 12.

Xu J, Wang J, Fan L, Li H, Zhang W, Hu Q, Jiang T (2015) Tractography-based parcellation of the human middle temporal gyrus. Scientific Reports 5.

Yerys BE, Tunç B, Satterthwaite TD, Antezana L, Mosner MG, Bertollo JR, Guy L, Schultz RT, Herrington JD (2019) Functional connectivity of frontoparietal and salience/ventral attention networks have independent associations with co-occurring attention-deficit/hyperactivity disorder symptoms in children with autism. Biological Psychiatry: Cognitive Neuroscience and Neuroimaging 4:343–351.

Yoo, H (2015) Genetics of Autism Spectrum Disorder: Current Status and Possible Clinical Applications. Experimental Neurobiology, 24(4), 257-272. doi: 10.5607/en.2015.24.4.257

Yu Y, Wang X, Yang J, Qiu J (2020) The role of the MTG in negative emotional processing in young adults with autistic-like traits: A fmri task study. Journal of Affective Disorders 276:890–897.

Zhao Y, Zhang L, Rütgen M, Sladky R, Lamm C (2021) Neural dynamics between anterior insular cortex and right supramarginal gyrus dissociate genuine affect sharing from perceptual saliency of pretended pain. eLife 10.

Zielinski BA, Andrews DS, Lee JK, Solomon M, Rogers SJ, Heath B, Nordahl CW, Amaral DG (2022) Sex-dependent structure of socioemotional salience, executive control, and default mode networks in preschool-aged children with autism. NeuroImage 257:119252.